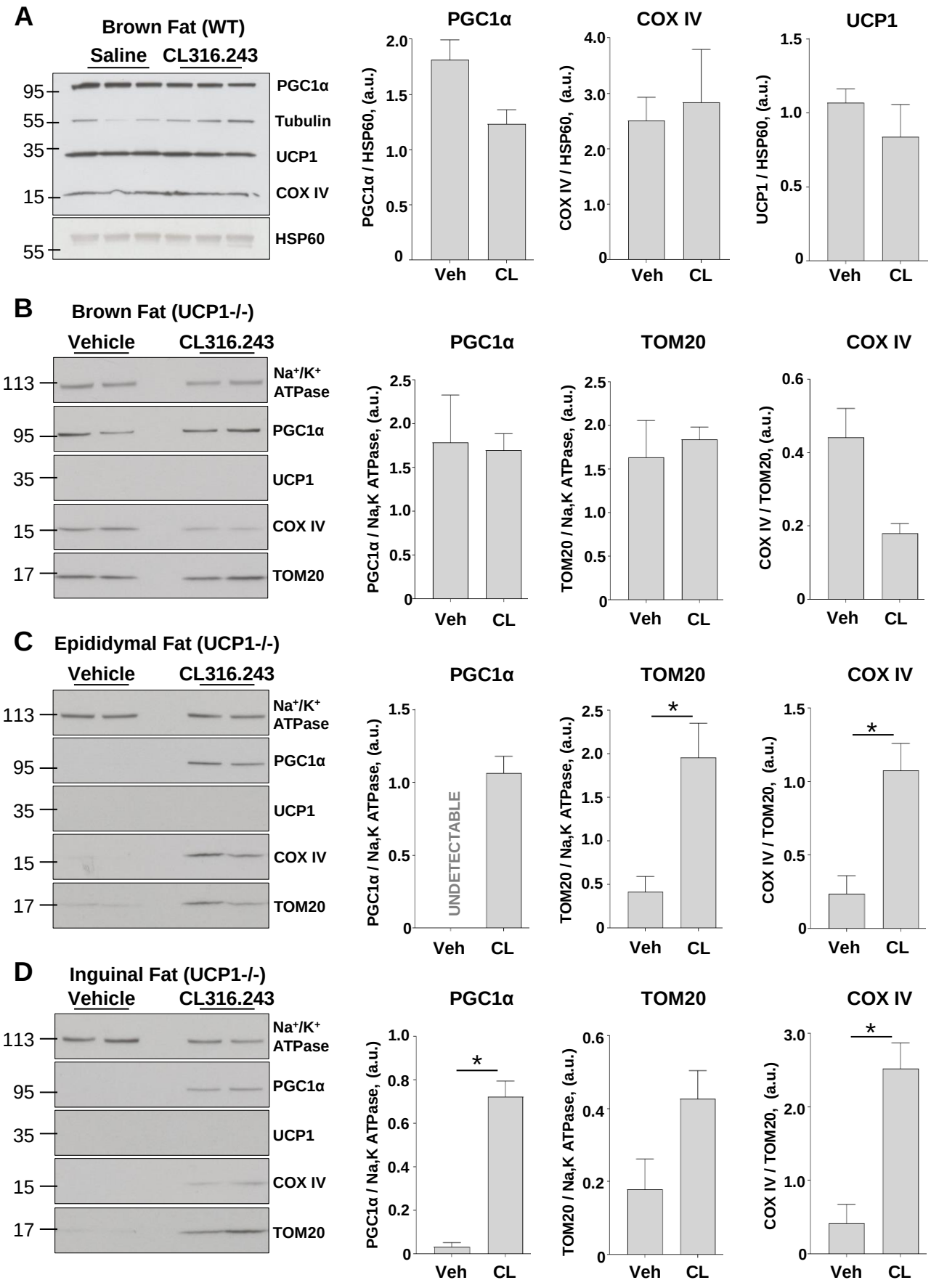

Figure S1. Effect of chronic β3-adrenergic receptor stimulation on brown adipose tissue. Related to Figure 1.

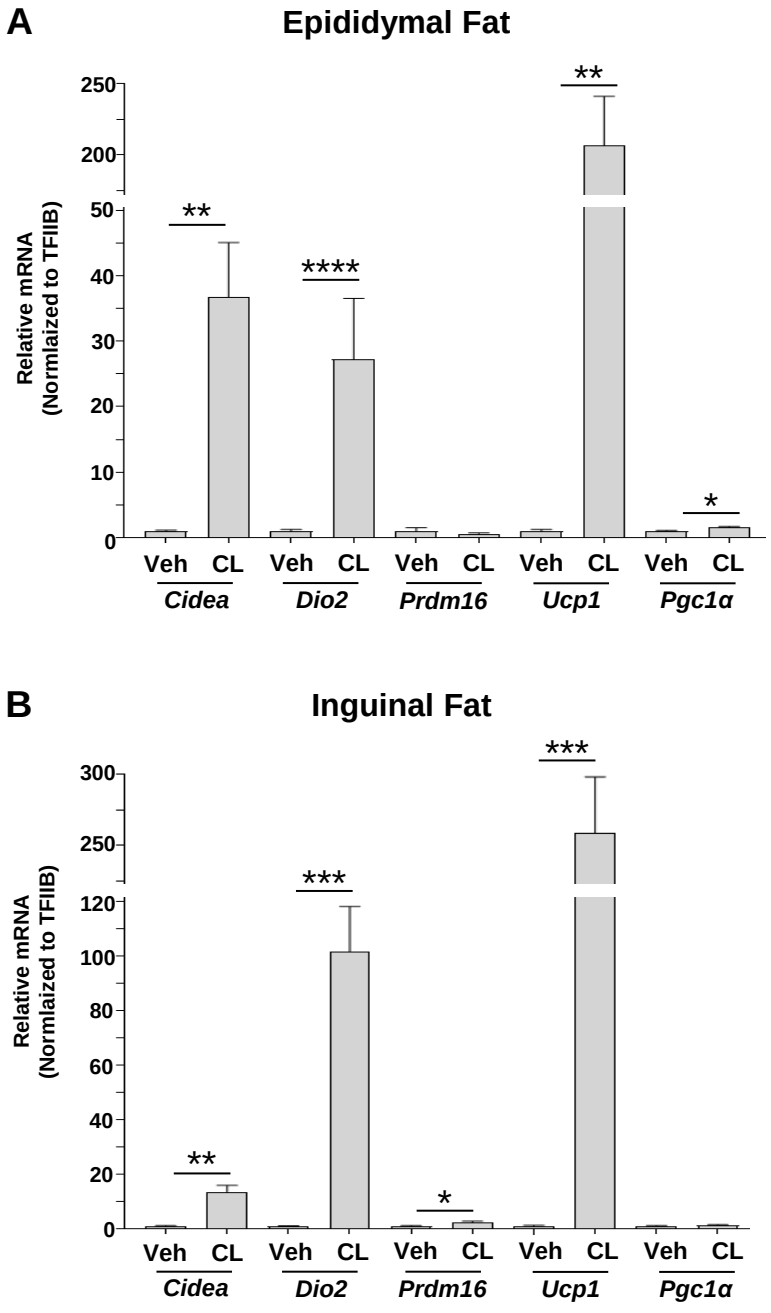

Figure S2. Thermogenic profile of epididymal and inguinal fat. Related to Figure 1

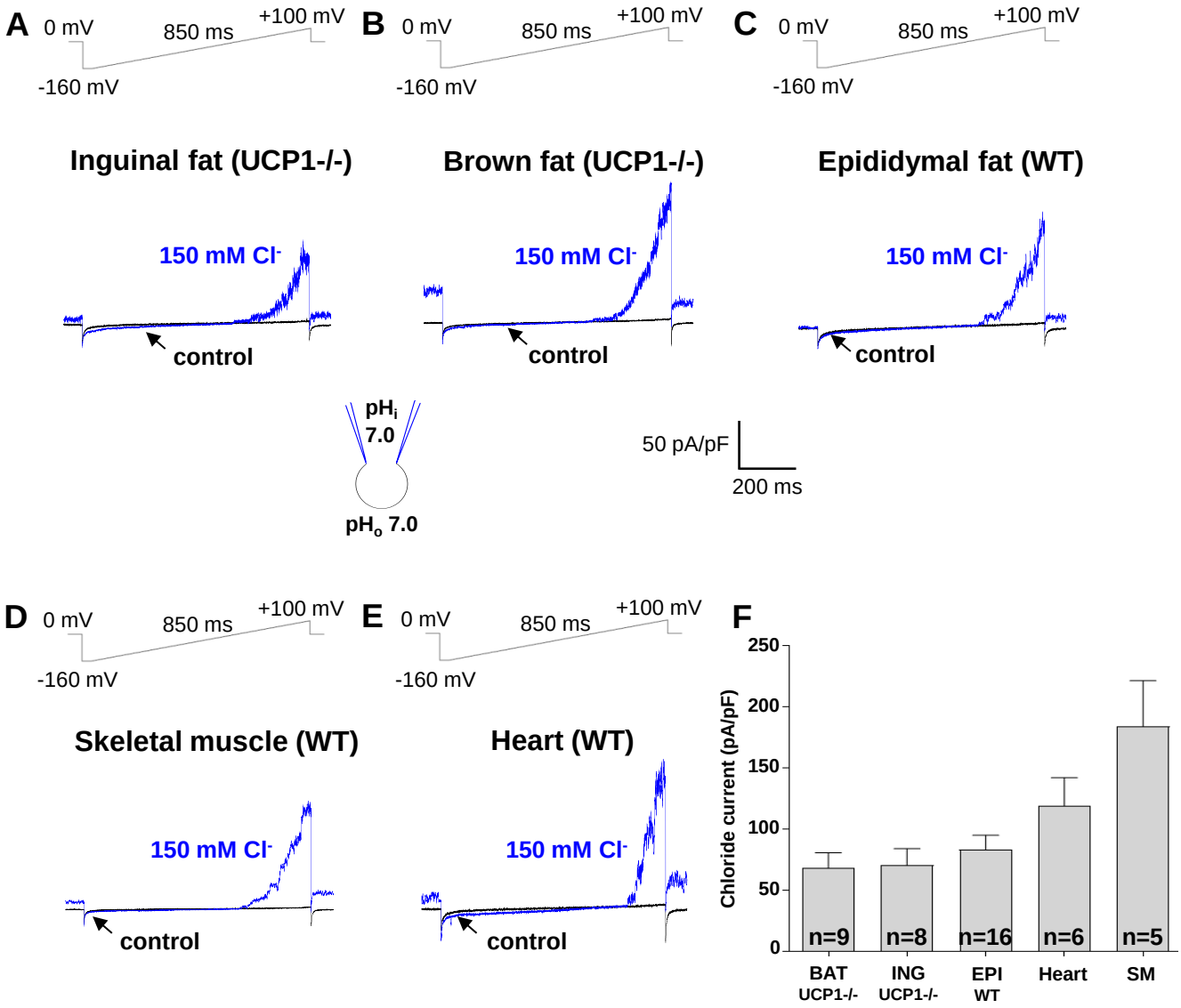

Figure S3. Mitochondrial Cl^- current in various mouse tissues. Related to Figure 3.

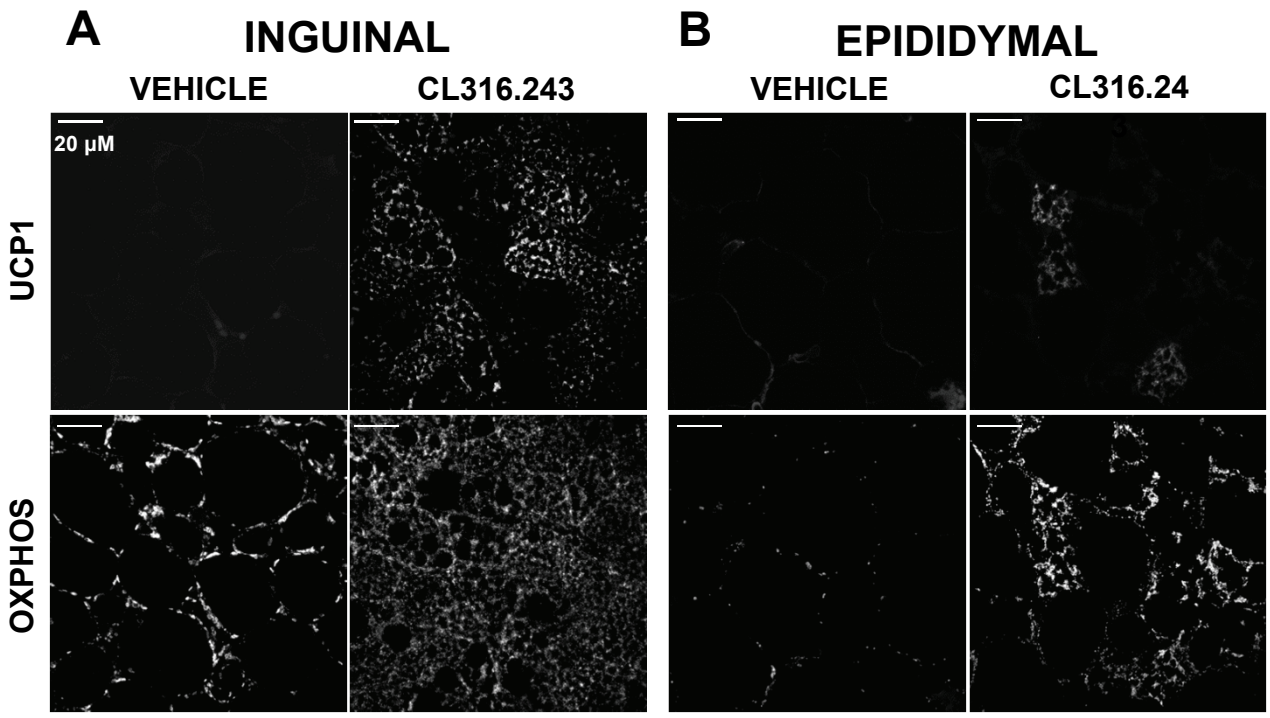

Figure S4. Mitochondrial biogenesis and UCP1 expression in inguinal and epididymal depots after chronic β3-adrenergic stimulation. Related to Figure 3.

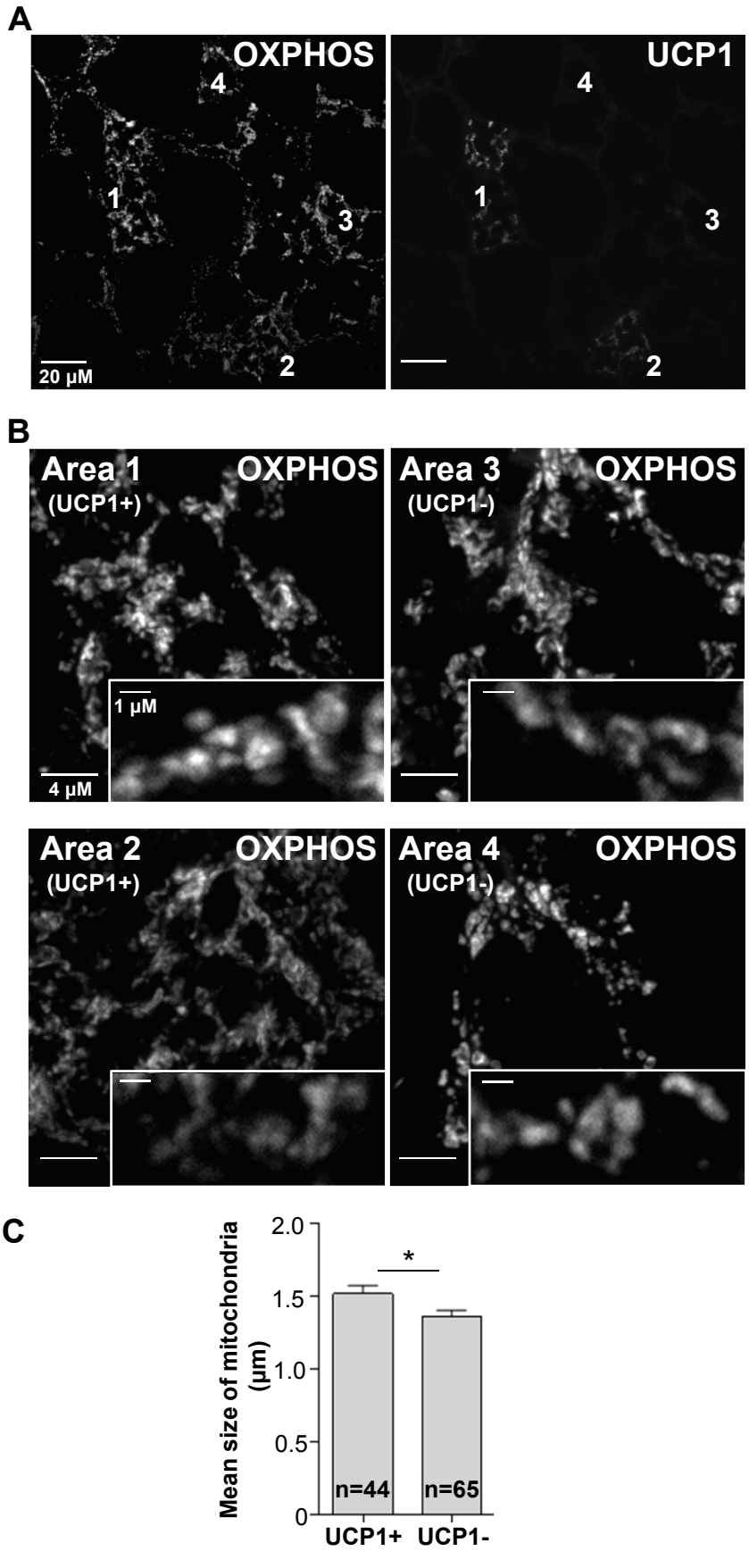

Figure S5. Mitochondrial size in UCP1+ and UCP1- beige adipocytes. Related to Figure 3

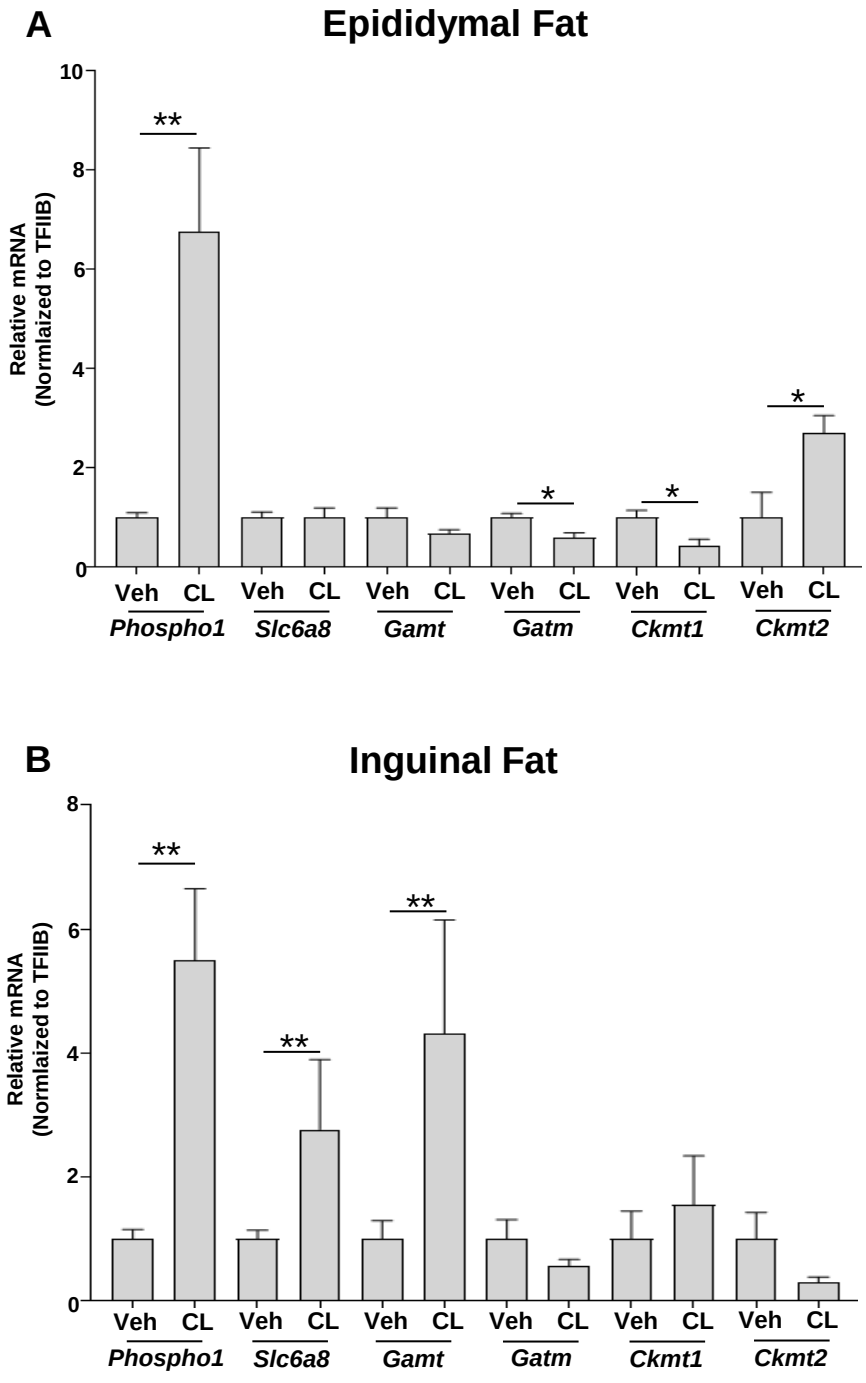

Figure S6. mRNA levels of proteins involved in creatine metabolism. Related to Figure 7

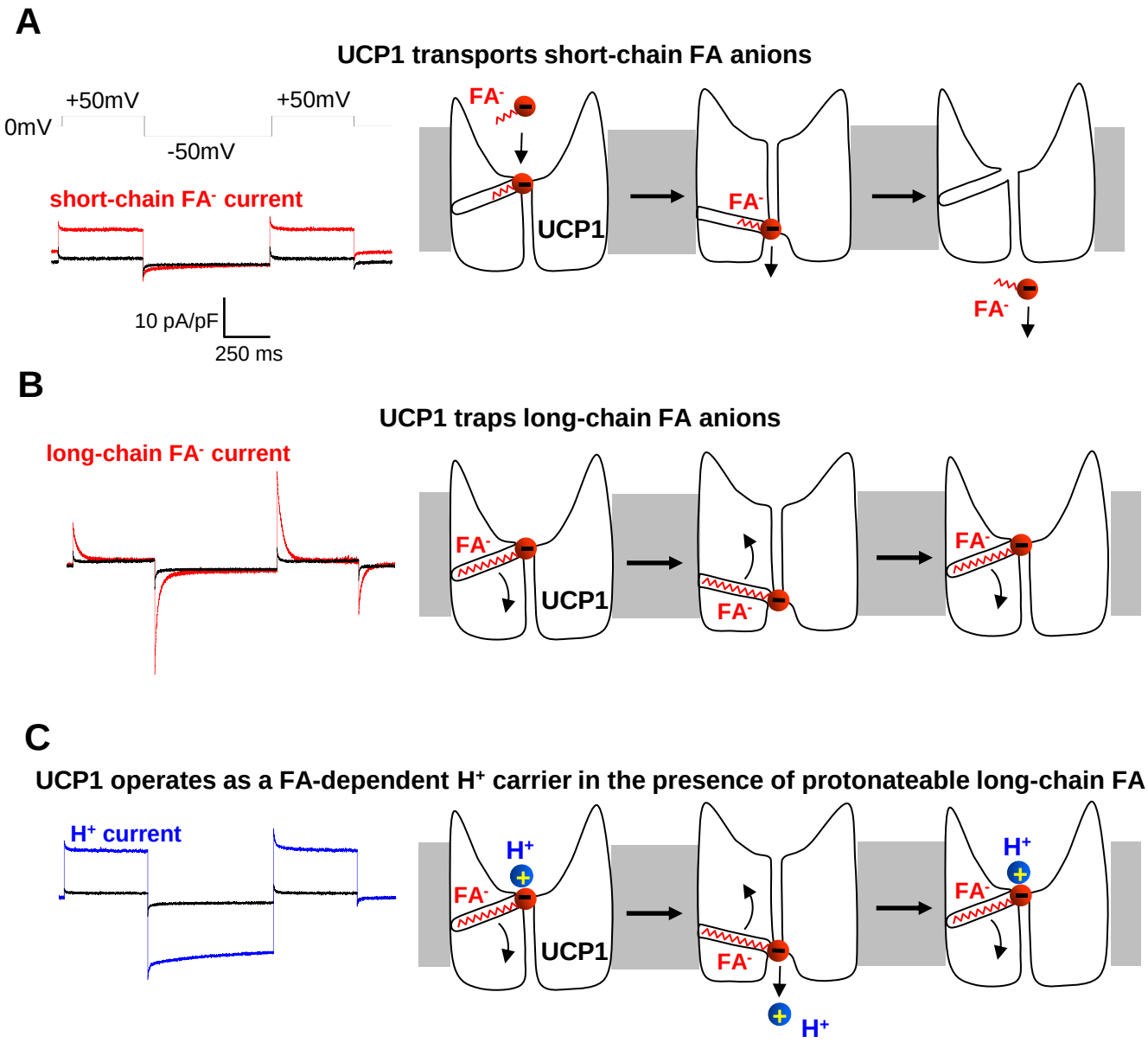

Figure S7. The mechanism by which FA control UCP1 currents in beige and brown fat. Related to Figure 4.

SUPPLEMENTAL FIGURE LEGENDS

Figure S1. Effect of chronic β3-adrenergic receptor stimulation on brown adipose tissue. Related to Figure 1

(A) Representative immunoblot showing the effect of β3-adrenergic receptor stimulation on the expression of Tubulin, PGC1α, UCP1, COX IV, and HSP60 proteins in brown fat. Histograms show PGC1α, COX IV and UCP1 protein levels relative to the levels of HSP60. Data shown as mean ± SEM, n = 3.

(B-D) Representative immunoblots showing the effect of β3-adrenergic receptor stimulation on the expression of Na^+/K^+ ATPase, PGC1α, UCP1, COX IV and TOM20 proteins in brown fat (B), inguinal fat (C), and epididymal fat (D) of UCP1-/- mice. Histograms show PGC1α, TOM20 and COX IV protein levels for each immunoblot (B-D). Data shown as mean ± SEM, n = 4.

Figure S2. Thermogenic profile of epididymal and inguinal fat. Related to Figure 1

Quantitative RT-PCR of *Cidea*, *Dio2*, *Prdm16*, *Ucp1*, *Pgc1α* from epididymal fat (A) and inguinal fat (B) showing the effect of β3-adrenergic receptor stimulation on the relative mRNA level for these genes. Data shown as mean ± SEM. n = 6 to 9.

Figure S3. Mitochondrial Cl^- current in various mouse tissues. Related to Figure 3.

(A-E) Representative Cl^- currents recorded in mitoplasts isolated from inguinal beige fat (UCP1-/-, A), brown fat (UCP1-/-, B), epididymal beige fat (UCP1-negative mitoplast, WT, C), skeletal muscle (WT, D), and heart (WT, E). Control traces were recorded in HEPES/Tris solution and Cl^- currents (blue) were induced by addition of KCl to the cytosolic face of the IMM (blue, see methods). The voltage protocol is indicated at the top.

(F) Bar graph showing average current density of Cl^- in brown fat (BAT, UCP1-/-), inguinal beige fat (ING, UCP1-/-), epididymal beige fat (EPI, UCP1-negative mitoplasts, WT), heart (WT), skeletal muscle (SM, WT). Data shown as mean ± SEM.

Figure S4. Mitochondrial biogenesis and UCP1 expression in inguinal and epididymal depots after chronic β3-adrenergic stimulation. Related to Figure 3.

(A and B) Confocal micrographs of inguinal fat and epididymal fat of mice treated with vehicle or CL316.243 and immunolabeled with UCP1 (upper panels) and with respiratory chain complex antibodies (MitoProfile® Total OXPHOS, lower panels); scale bar, 20 μm).

Figure S5. Mitochondrial size in UCP1+ and UCP1- beige adipocytes. Related to Figure 3

(A) A representative confocal micrograph of epididymal fat of CL-treated mice, immunolabeled with respiratory chain complex antibodies (MitoProfile® Total OXPHOS, left panel) and with UCP1 antibody (right panel); scale bar, 20 μm.

(B) Magnified views of areas 1 and 2 (UCP1 positive adipocytes), and areas 3 and 4 (UCP1 negative adipocytes) of panel A. Mitochondrial networks are shown.

(C) Histogram showing the mean size of mitochondria of UCP1 positive (UCP1+) and UCP1 negative (UCP1-) adipocytes based on panel B. Data shown as mean ± SEM.

Figure S6. mRNA levels of proteins involved in creatine metabolism. Related to Figure 7

(A and B) Quantitative RT-PCR of *Phospho1*, *Slc6a8*, *Gamt*, *Gatm*, *Ckmt1* and *Ckmt2* from epididymal (A) and inguinal fat (B), showing the effect of β3-adrenergic receptor stimulation. Data shown as mean ± SEM. n = 6 to 9.

Figure S7. The mechanism by which FA control UCP1 currents in beige and brown fat. Related to Figure 4

(A) *Right panel:* an example of steady UCP1 current induced by short-chain low-pKa FA analogs added on the cytosolic face of the IMM. Voltage protocol is shown above. *Left panel:* the mechanism of this current. Short-chain FA- are transported by UCP1 across the IMM.

(B) *Right panel:* an example of transient UCP1 current induced by long-chain low-pKa FA analogs added on the cytosolic face of the IMM. *Left panel:* the mechanism of this current. A long-chain FA^- analog is translocated by UCP1 similar to short-chain FA^-, however the long carbon tail of FA^- establishes strong hydrophobic interaction with UCP1 to prevent FA^- dissociation. Thus, the negatively charged FA^- shuttles within the UCP1 translocation pathway in response to the transmembrane voltage, producing transient currents.

(C) *Right panel:* an example of steady H^+ current via UCP1 induced by regular long-chain FA added on the cytosolic face of the IMM. *Left panel:* the mechanism of this current. UCP1 operates as a symporter that transports one FA^- and one H^+ per the transport cycle. The H^+ and the FA^- are translocated by UCP1 upon conformational change, and H^+ is released on the opposite side of the IMM, while the FA^- stays associated with UCP1 due to the hydrophobic interactions established by its carbon tail. The FA^- anion then returns to initiate another H^+ translocation cycle. Charge is translocated only in step 3 when the LCFA anion returns without the H^+.